Reactivities and Collision-Induced Dissociation of Vanadium Oxide Cluster Cations

R. C. Bell, K. A. Zemski, K. P. Kerns, H. T. Deng, and A. W. Castleman, Jr.*

Department of Chemistry, The Pennsylvania State University, University Park, Pennsylvania 16802

Received: October 24, 1997; In Final Form: December 31, 1997

Reactivities and collision-induced dissociation of vanadium oxide cluster cations are investigated using a triple quadrupole mass spectrometer coupled with a laser vaporization source. The dominant peaks in the mass distribution correspond to cluster ions with stoichiometries of $(VO_2)_n(V_2O_5)_m(O_2)_q^+$. Collision-induced dissociation studies of the vanadium oxide species $V_2O_{4-6}^+$, $V_3O_{6-9}^+$, $V_4O_{8-10}^+$, $V_5O_{11-13}^+$, $V_6O_{13-15}^+$, and $V_7O_{16-18}^+$ show that VO_2, VO_3, and V_2O_5 units are the main building blocks for most of these clusters. The reaction pathways observed for these vanadium oxide clusters include molecular association, cracking, dehydration, and oxygenation of the neutral hydrocarbons with the reactivities of specific clusters differing from species to species. For example, $V_3O_7^+$ is very efficient in the dehydrogenation of 1,3-butadiene and in the cracking of 1-butene. On the other hand, $V_3O_6^+$ produces only molecular association products with these same reactants. To help explain these differences in reactivity, calculations on the molecular structure of some of these cluster ions were also undertaken, and the findings are presented.

Introduction

Transition metal oxides are becoming increasingly important in catalysis because of their ability to effect oxidation−reduction reactions while, at the same time, being cost-efficient and in many cases environmentally benign. Supported metal catalysts have been extensively used in the chemical industry, and in the past, the oxides have traditionally been viewed as an inert support for the active catalyst. It has now been established that the support can influence the activity and selectivity of various catalytic processes in a variety of ways. These interactions may be caused by the support leading to a stabilization of unique structures of the catalyst, changing the electronic properties due to electron-transfer processes between the metal particles and the support, or by compound formation between the metal and support.[1] Early transition metal oxides, such as titanium and vanadium oxides, are now being used as supports for numerous catalytic processes and in many cases are found to be useful catalysts themselves. For example, vanadium oxide catalysts[2−4] have been used in many industrial applications, such as the production of sulfuric acid[5] and in the selective oxidation and ammoxidation of aromatic hydrocarbons.[6,7] Many studies have been performed to gain insight into the mechanism for oxovanadium catalysis.[8−10] Other spectroscopic studies have given insight into the electronic structure of the so-called pseudotetrahedral oxovanadium groups.[11]

Mixed metal oxide catalysts are also becoming prevalent. For example, Topsøe has investigated the selective catalytic reduction of nitric oxide by ammonia using vanadia−titania catalysts.[12] Also, the use of vanadyl pyrophosphate in oxidation reactions has spurred great interest in the chemical community.[13] For example, DuPont recently has implemented vanadium phosphorus oxides (VPO) as catalysts in the production of maleic anhydride from *n*-butane.[14] Understanding the nature of the reactive sites in heterogeneous catalysis can be aided by gas-phase studies of neutral and ionic clusters, in addition to studies of these materials in solids or solutions. Ultimately, comparison of the results can provide insight into the effects of stoichiometry, charge, and oxidation state of catalytic reactions.

In many cases it is useful to view the surface structure of the bulk as an assemblage of clusters of different sizes and isomers.[15] It is less difficult to probe the properties of gas-phase clusters than it is to study the surface of the bulk solid, and in many cases findings in this area substantially contribute to a greater understanding of the catalytic dependence on the local surface structure. For example, Staley et al. have studied the oxidation of carbon monoxide by transition metal cations.[16] The reactivities of bare transition metals (M^+) and their monoxides (MO^+) toward both saturated and unsaturated hydrocarbons have been investigated.[17,18] Schwarz and co-workers have found that some of the more reactive transition metal oxides (e.g., FeO^+ and PtO^+) can even activate methane,[17b] from which a highly selective route to produce methanol has been long sought. Freiser and co-workers have studied the gas-phase reactions of V^+ and VO^+ with small alkanes using Fourier transform mass spectrometry; dehydrogenation of these hydrocarbons was found to predominate, although cracking was observed in reactions of the larger species investigated (C_nH_{2n+2}, $n \geq 5$).[19]

Although much has been accomplished through investigations of bare metal and monomeric metal oxides in the gas phase, very few studies on the reactivities and dissociation of transition metal oxide clusters have been undertaken. Studies of titanium oxide clusters have focused on their reactivities toward molecular oxygen,[20] as well as their structures, based on both calculations and collision-induced dissociation products.[21] Over the past several years, investigations into the reactivities of transition metal oxides have been sparse. Indeed, to the best of our knowledge, Zamaraev and co-workers are the only other research group that have attempted to correlate results for metal oxide cluster ions with known behavior for real catalysts.[22] Their work was based on similarities between reactions of methanol

S1089-5639(97)03453-1 CCC: $15.00
Published on Web 02/12/1998

with molybdenum oxide cluster cations compared to that of the real catalysts in the bulk phase.

Recently, Castleman and co-workers have conducted studies on niobium oxide cluster ions, focusing on cluster ion distributions, collision-induced dissociation (CID) studies, and ab initio calculations.[23] These studies provided strong evidence for specific structures, including approximations of bonding energies and ionization energies for certain clusters. Novel reactivities were observed for some of these clusters, including findings of clusters containing reactive oxygen centers, which may be useful in the development of new catalytic processes.

The present studies focus on the reactivities and collision-induced dissociation of vanadium oxide cluster cations. Their observed reactivities toward industrially important hydrocarbon gases, such as *n*-butane (C_4H_{10}), 1-butene (C_4H_8), and 1,3-butadiene (C_4H_6), differ greatly from similar reactivity studies made on niobium oxide cluster ions.[23] Although niobium and vanadium are both in group VA, vanadium oxide clusters are much more active in selectively breaking bonds of these hydrocarbon reactants. Even though the mass distributions of the oxide cluster ions are different for niobium and vanadium, the products formed from collision-induced dissociation (CID) are nearly identical, indicating a similarity in the overall structures.

Experimental Section

The experiments reported herein were conducted using a triple quadrupole mass spectrometer coupled with a laser vaporization source (TQMS-LV), which has been described previously.[23−25] Briefly, the second harmonic output of a Nd:YAG laser is focused onto a small spot to ablate the surface of a rotating and translating vanadium rod. Pulses of a mixture of O_2 seeded in helium (ca. 10%) are injected by a pulsed valve and directed over the ablating rod surface, during which time plasma reactions take place. As a result, vanadium oxide clusters of various sizes are produced that thereafter undergo supersonic expansion as they exit the laser vaporization source. After the clusters enter the main chamber through a skimmer, the cluster ions are focused and steered by a group of ion lenses and deflectors. These ions then enter the first quadrupole mass filter, which enables the selection of species of one particular mass from the total ion mass distribution in order to individually study its reactivity or CID behavior. The selected cluster ions are then guided by a second group of ion lenses into the second quadrupole mass spectrometer operated in the rf-only mode, which serves as either a reaction or collision cell. Herein, investigations of both the reactivities and collision-induced dissociation of selected clusters take place. The pressure in the collision cell is monitored by a capacitance manometer. In the reaction studies, the translational energy is kept to a minimum by applying either ground potential or a slightly repulsive potential to the second quadrupole rods and the entrance plate of the collision cell in order to introduce only thermal ions into the reaction region. These precautions ensure that the observed reactions take place at or very near thermal energies. Following ensuing collisional processes, including reactions, the product ions exit the second quadrupole. Thereafter, they are refocused by a third group of ion lenses into the third quadrupole mass filter affixed with a channeltron electron multiplier, where the ion mass products are detected for analysis.

Results

Cluster Distribution and Dissociation. The total cluster ion distribution resulting from laser plasma reactions of vanadium with molecular oxygen (∼10% seeded in helium) is shown in Figure 1a. The first prominent peak in the cluster distribution begins with the monooxide VO^+. Each set of peaks corresponds to clusters having a particular number of vanadium atoms, and the difference in mass between each peak of a set corresponds to one oxygen atom. Overall, the major peaks observed are $V_2O_{4-8}^+$, $V_3O_{6-9}^+$, $V_4O_{8-12}^+$, $V_5O_{11-13}^+$, $V_6O_{13-17}^+$, and $V_7O_{15-18}^+$; in other words, clusters with stoichiometries of $(VO_2)_n(V_2O_5)_m(O_2)_{0-2}^+$, or alternatively $(VO_2)_x(VO_3)_y(O_2)_{0-3}^+$, are dominant in the cluster distribution. This finding is consistent with the stoichiometry of bulk vanadium oxide, which is found to be composed of VO_2 and V_2O_5 units.[26] As a result, the collision-induced dissociation and reactivities of these dominant cluster ions are the focus of this study. Furthermore, clusters having an even number of vanadium atoms generally have a greater number of peaks with higher oxygen content in the cluster series than those with an odd number of vanadium atoms. Varying the percentage of O_2 seeded in the helium carrier gas in the range between 6 and 30% had little effect on the mass distribution. Below this percentage of O_2 in helium, peaks corresponding to the clusters of higher ratios of metal to oxygen appear with minor intensity, for example, $V_2O_3^+$ and $V_5O_{10}^+$. But, the intensity of all peaks began to decrease.

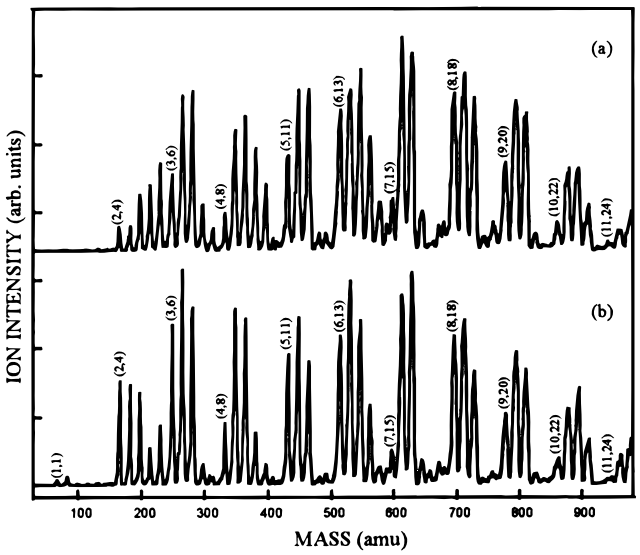

Figure 1. Total ion mass distribution of vanadium oxide cluster cations. The numbers in parentheses, (*x*,*y*), denote the number of vanadium and oxygen atoms in the cluster $V_xO_y^+$; the remaining peaks correspond to masses with an additional oxygen atom as a series progresses. Spectra in (a) display the mass distribution from the laser plasma reactions of vanadium with 10% oxygen seeded in the helium carrier gas. The same conditions were used to generate the cluster distribution in (b); however, 0.4 mTorr of krypton was added to the collision cell to determine the most stable cations.

In one series of experiments, the collision-induced dissociation (CID) behavior of several metal oxide clusters with varying metal-to-oxygen ratios was studied in order to gain insight into their formation mechanisms and structures. Xenon was used to perform CID on the clusters $V_2O_{4-6}^+$, $V_3O_{6-9}^+$, $V_4O_{8-10}^+$, $V_5O_{11-13}^+$, $V_6O_{13-15}^+$, and $V_7O_{16-18}^+$. Table 1 displays a summary of the CID products for $V_{2-4}O_y^+$, and the CID products for the clusters $V_{5-7}O_y^+$ are presented in Table 2. The findings show that $V_2O_4^+$, $V_3O_{6,7}^+$, $V_4O_{8,9}^+$, $V_5O_{11,12}^+$, $V_6O_{13,14}^+$, and $V_7O_{16,17}^+$ are very stable species, requiring about 3−5 eV (center-of-mass reference frame) of energy at single-collision conditions to initiate dissociation. For the clusters $V_3O_6^+$, $V_4O_8^+$, and $V_5O_{11}^+$, the main CID product is VO^+, while for

TABLE 1: CID Fragmentation Channels of Selected $V_{2-4}O_y^+$ Clusters[a]

selected ion $V_xO_y^+$	CID product (cations)	neutral(s) lost[d]	selected ion $V_xO_y^+$	CID product (cations)	neutral(s) lost[d]
2,4	1,2	1,2	3,9	3,7	0,2[b]
	1,1	1,3		1,2	2,7[c]
2,5	2,4	0,1	4,8	1,1	3,7
	1,2	1,3		3,6	1,2
	2,3	0,2		2,4	2,4
2,6	2,4	0,2[b]	4,9	1,2	3,7
	1,2	1,4[c]		2,4	2,5
3,6	1,1	2,5		3,6	1,3
	2,4	1,2		3,7	1,2
	1,2	2,4	4,10	4,8	0,2[b]
3,7	1,2	2,5		3,7	1,3
	2,4	1,3		1,1	3,9[c]
	1,1	2,6[c]		1,2	3,8[c]
3,8	3,6	0,2[b]			
	1,1	2,7[c]			
	2,4	1,4[c]			

[a] Note: Fragmentation channels are shown in order of observation with increasing collision energy. [b] Represents that dissociation occurs at near thermal energies. [c] Describes channels taking place under multiple collision conditions. [d] The neutral loss is assigned based on the difference between the selected cluster and fragment ion formed.

TABLE 2: CID Fragmentation Channels of Selected $V_{5-7}O_y^+$ Clusters[a]

selected ion $V_xO_y^+$	CID product (cations)	neutral(s) lost[d]	selected ion $V_xO_y^+$	CID product (cations)	neutral(s) lost[d]
5,11	1,1	4,10	6,15	6,13	0,2[b]
	2,4	3,7		5,12	1,3
	3,6	2,5		2,5	4,10
5,12	1,2	4,10		3,6	3,9[c]
	3,7	2,5	7,16	3,6	4,10
5,13	5,11	0,2[b]		4,9	3,7
	1,1	4,12		2,4	5,12
6,13	3,6	3,7		1,1	6,15[c]
	1,1	5,12		1,2	6,14[c]
	2,4	4,9	7,17	3,7	4,10
	2,3	4,10		1,2	6,15
6,14	2,4	4,10	7,18	7,16	0,2[b]
	1,2	5,12			
	3,7	3,7			

[a] Note: Fragmentation channels are shown in order of observation with increasing collision energy. [b] Represents that dissociation occurs at near thermal energies. [c] Describes channels taking place under multiple collision conditions. [d] The neutral loss is assigned based on the difference between the selected cluster and fragment ion formed.

the clusters $V_2O_4^+$, $V_3O_7^+$, $V_4O_9^+$, and $V_5O_{12}^+$, the major product ion is the VO_2^+ unit. The clusters of higher oxygen content, $V_2O_6^+$, $V_3O_{8,9}^+$, $V_4O_{10}^+$, $V_5O_{13}^+$, $V_6O_{15}^+$, and $V_7O_{18}^+$, lose molecular oxygen near thermal energies and single-collision conditions. For the larger clusters, $V_6O_{13,14}^+$ and $V_7O_{16,17}^+$, minor channels corresponding to VO^+ and VO_2^+ are observed, but larger metal oxide fragments are the predominant CID products. The clusters of higher oxygen content appear to be the stable clusters mentioned above, with additional O_2 units attached. For example, it is proposed that the $V_3O_8^+$ is composed of O_2 chemisorbed to the surface of the $V_3O_6^+$ cluster. This assumption is made due to the ease with which O_2 units are lost. While the CID results indicate that VO_2, V_2O_5, and VO_3 units are the dominant neutrals lost from certain clusters, it should be noted that we are unable to actually detect these neutrals; we only assume that these neutral clusters are intact under single-collision conditions at the collision energies used.

To determine the most stable cations in the mass distribution,

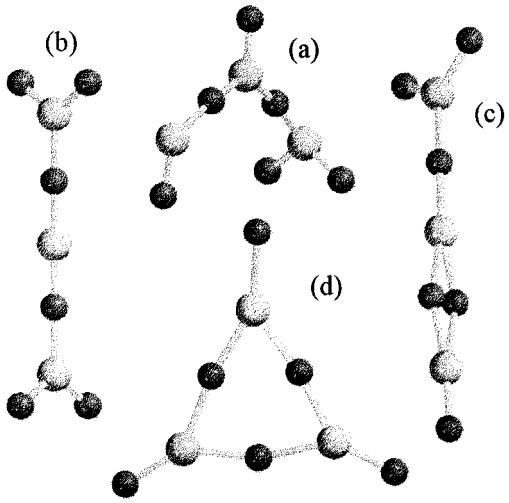

Figure 2. Proposed structures for the cluster $V_3O_6^+$.

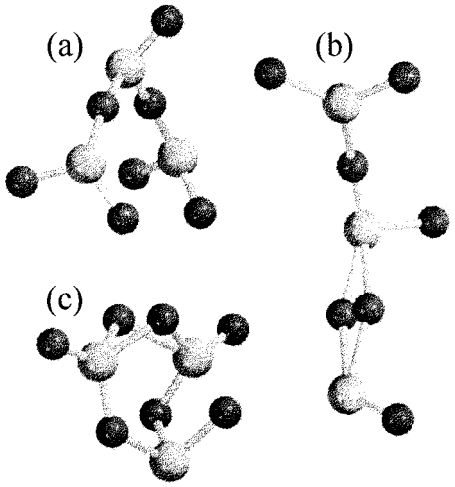

Figure 3. Proposed structures for the cluster $V_3O_7^+$.

0.4 mTorr of krypton and 6 eV (laboratory reference frame) of collision energy were used to collect a mass distribution as shown in Figure 1b, whereas xenon was used to determine the collision-induced dissociation products. It is observed from comparison with Figure 1a (the mass distribution without krypton in the collision cell) that a minor shift to the metal-rich clusters occurs although no new peaks are observed in the spectrum. These findings, along with studies of reactions, and in some cases calculations, are employed to infer reasonable structural models of these clusters as discussed later in the paper.

Cluster Structures and Properties by ab Initio Calculations. Ab initio calculations are performed for the clusters $V_3O_6^+$ and $V_3O_7^{0/+}$ using Spartan 4.0 software[27] on an IBM RISC 6000 model 550 computer in our laboratory. The cluster structures are optimized at the Hartree−Fock level using a 3-21G* polarization basis set. Although such molecules cannot be adequately treated at the level of theory used, the calculations allow some insight into the possible structures that may exist and assist in interpretation of the findings. The possible structures for $V_3O_6^+$ are shown in Figure 2. The structures in (a) and (b) have been optimized, whereas the other two structures have not yet been optimized. The difference in energies between structures (a) and (b) is approximately 322 kJ/mol with structure (a) being the more stable cluster cation. The possible structures for the cluster $V_3O_7^+$ are shown in Figure 3 where (a) and (c) are optimized; it should be noted that (b) is not yet optimized. The difference in energy for the clusters

TABLE 3: Reactions of Vanadium Oxide Cluster Cations $V_{2-3}O_y^+$ with 0.3 mTorr of *n*-Butane, 1-Butene, and 1,3-Butadiene

cluster $V_xO_y^+$ (x,y)	reactant gas								
			n-butane (C_4H_{10})			1-butene (C_4H_8)			1,3-butadiene (C_4H_6)
	a	*b*		*a*	*b*		*a*	*b*	
(2,4)	W	C	$(2,4)^+ \cdot C_2H_4$	W	C	$(2,4)^+ \cdot CH_2$	W	C	$(2,4)^+ \cdot C_2H_3$
	M	C	$(2,3)^+ \cdot C_2H_8$	D	C	$(2,4)^+ \cdot C_2H_4$	M	C	$(2,3)^+ \cdot C_4H_4$
	D	B	$(2,4)^+ \cdot C_4H_{10}$	W	C	$(2,3)^+ \cdot C_4H_6$	D	A	$(2,4)^+ \cdot C_4H_6$
				M	C	$(2,4)^+ \cdot C_4H_8$			
(2,5)	D	B	$(2,4)^+$	W	C	$(2,3)^+$	M	C	$(2,3)^+$
	W	C	$(2,4)^+ \cdot C_2H_4$	D	A	$(2,4)^+$	D	A	$(2,4)^+$
	M	C	$(2,5)^+ \cdot C_2H_4$	S	B	$(2,4)^+ \cdot C_2H_4$	W	C	$(2,4)^+ \cdot C_2H_3$
	W	C	$(2,4)^+ \cdot C_4H_{10}$	W	C	$(2,5)^+ \cdot C_2H_4$	W	C	$(2,3)^+ \cdot C_4H_4$
	W	C	$(2,5)^+ \cdot C_4H_{10}$	W	C	$(2,4)^+ \cdot C_4H_8$	M	C	$(2,3)^+ \cdot C_4H_6$
				M	C	$(2,5)^+ \cdot C_4H_8$	M	C	$(2,5)^+ \cdot C_2H_3$
							W	C	$(2,4)^+ \cdot C_4H_4$
							M	C	$(2,4)^+ \cdot C_4H_6$
							W	C	$(2,5)^+ \cdot C_4H_6$
(2,6)	M	C	$(2,4)^+$	M	B	$(2,4)^+$	M	B	$(2,4)^+$
	W	C	$(2,5)^+$	W	C	$(2,5)^+$	W	C	$(2,5)^+$
	D	B	$(2,4)^+ \cdot C_4H_{10}$	D	A	$(2,4)^+ \cdot C_4H_8$	D	A	$(2,4)^+ \cdot C_4H_6$
	W	C	$(2,6)^+ \cdot C_4H_{10}$						
(3,6)	W	C	$(3,6)^+ \cdot C_2H_4$	D	C	$(3,6)^+ \cdot C_4H_8$	D	B	$(3,6)^+ \cdot C_4H_6$
	D	C	$(3,6)^+ \cdot C_4H_{10}$						
(3,7)	W	C	$(3,6)^+$	M	C	$(3,6)^+$	W	C	$(3,6)^+$
	M	C	$(3,7)^+ \cdot C_2H_4$	D	C	$(3,7)^+ \cdot C_2H_4$	M	A	$(3,6)^+ \cdot C_4H_4$
	D	C	$(3,7)^+ \cdot C_4H_{10}$	W	C	$(3,6)^+ \cdot C_4H_6$	D	A	$(3,7)^+ \cdot C_4H_6$
				W	C	$(3,7)^+ \cdot C_4H_8$			
(3,8)	M	C	$(3,6)^+$	M	C	$(3,6)^+$	D	B	$(3,6)^+$
	D	C	$(3,7)^+$	D	B	$(3,7)^+$	M	B	$(3,7)^+$
	W	C	$(3,6)^+ \cdot C_4H_{10}$	W	C	$(3,7)^+ \cdot C_2H_4$	W	C	$(3,6)^+ \cdot C_4H_6$
	W	C	$(3,7)^+ \cdot C_4H_{10}$	W	C	$(3,6)^+ \cdot C_4H_8$	W	C	$(3,7)^+ \cdot C_4H_6$
	W	C	$(3,8)^+ \cdot C_4H_{10}$	W	C	$(3,7)^+ \cdot C_4H_8$	W	C	$(3,8)^+ \cdot C_4H_6$
				W	C	$(3,8)^+ \cdot C_4H_8$			

[a] These columns represent the product intensity with respect to the other peaks in that particular spectrum with each product marked as the dominant (D) product of the reaction or as strong (S), moderate (M), or weak (W) product ions. [b] These columns represent the product intensity with respect to all of the cluster reactions studied with each product marked as strong (A), moderate (B), or weak (C).

shown in (a) and (c) is 219 kJ/mol with the structure in (c) being slightly more stable. Other suggested structures that are in accord with our experimental observations (some of which are displayed later in this paper) have not yet been optimized and will be presented in a future paper.

Reactivities with Butane, Butene, and Butadiene. In the present experiments, great emphasis is placed on the reactivities of alkanes and alkenes toward vanadium oxide cluster ions. Specifically, the reactivities of various vanadium oxide cluster ions with four-carbon-containing hydrocarbons, namely *n*-butane, 1-butene, and 1,3-butadiene, were studied at pressures between 0.1 and 0.7 mTorr near thermal energies. Generally, the reactivities of saturated hydrocarbons are found to be lower than those of unsaturated species with the selected clusters. Interestingly, the differences in the reactivities of $V_3O_6^+$ and $V_3O_7^+$ have potentially significant implications regarding catalytic activity.

In the case of *n*-butane, molecular association is the dominant reaction channel for most of the clusters studied. Also, the majority of the clusters studied display single oxygen loss from the cluster when reacted with the hydrocarbons; exceptions are $V_2O_4^+$, $V_3O_6^+$, $V_4O_8^+$, $V_5O_{11}^+$, $V_6O_{13}^+$, and $V_7O_{16}^+$ which display no oxygen loss at reactant gas pressures of up to 0.3 mTorr. For the clusters $V_2O_5^+$, $V_3O_7^+$, $V_4O_9^+$, $V_5O_{12}^+$, $V_6O_{14}^+$, and $V_7O_{17}^+$, single oxygen loss was observed for reactions with most of the hydrocarbons studied at single-collision conditions near thermal energies. The results can be seen in Tables 3 and 4 which represent reactions at reactant gas pressures of 0.3 mTorr. The first column to the right of each set of reactions indicates the intensity with which these products occur in accordance with that particular spectrum. The second column to the right of each set of reactions indicates the intensity of those products with respect to all the clusters examined. These reactions are unique because the CID results under single-collision conditions near thermal energies displayed no oxygen atom loss for any cluster in the mass distribution with the exception of $V_2O_5^+$, and no molecular or atomic oxygen loss was observed for the clusters mentioned above. However, those clusters with ligated molecular oxygen ($V_2O_6^+$, $V_3O_8^+$, $V_4O_{10}^+$, $V_5O_{13}^+$, $V_6O_{15}^+$, and $V_7O_{18}^+$) are found to react somewhat differently. Those clusters that facilely lose O_2 may associate *n*-butane, but the predominant reaction channel is loss of atomic and molecular oxygen under single-collision conditions; peaks that correspond to the association products of these clusters also appear in the spectrum at higher pressures. Minor channels for C2−C3 cracking were observed for the clusters $V_2O_{4,5}^+$, $V_3O_{6,7}^+$, and $V_5O_{11,12}^+$. In addition, minor products representing the dehydration of the $V_2O_4^+$ and $V_2O_5^+$ association products were also observed, but this channel was not observed for any of the other clusters.

The reactions of the vanadium oxide cluster ions with 1-butene display a dominant molecular association reaction pathway. The same phenomena for the abstraction of oxygen from the selected cluster that was previously described is observed in the cluster reactions with 1-butene as seen in Tables 3 and 4. The clusters $V_2O_{4,5}^+$, $V_3O_7^+$, and $V_5O_{12}^+$ are able to break the C2−C3 bond (single bond) of 1-butene. However, association is the dominant channel for the $V_2O_{4,5}^+$ and $V_5O_{12}^+$ clusters, while cracking dominates the reaction pathway of $V_3O_7^+$ as seen in Figure 4. On the other hand, the clusters $V_3O_6^+$ and $V_5O_{11}^+$ are totally inert to the breaking of bonds for 1-butene and only show a molecular association reaction channel. The clusters $V_2O_{4,5}^+$ and $V_3O_7^+$ also display a minor channel for the dehydration of their association products.

TABLE 4: Reactions of Vanadium Oxide Cluster Cations $V_{4-7}O_y^+$ with 0.3 mTorr of *n*-Butane, 1-Butene, and 1,3-Butadiene

cluster $V_xO_y^+$ (x,y)	reactant gas								
			n-butane (C_4H_{10})			1-butene (C_4H_8)			1,3-butadiene (C_4H_6)
	a	*b*		*a*	*b*		*a*	*b*	
(4,8)			no reaction	D	C	$(4,8)^+ \cdot C_4H_8$	D	C	$(4,8)^+ \cdot C_4H_6$
(4,9)	W	C	$(4,8)^+$	W	C	$(4,8)^+$	W	C	$(4,8)^+$
	D	C	$(4,9)^+ \cdot C_4H_{10}$	D	C	$(4,9)^+ \cdot C_4H_8$	D	C	$(4,9)^+ \cdot C_4H_6$
(4,10)	W	C	$(4,8)^+$	W	C	$(4,8)^+$	M	C	$(4,8)^+$
	D	C	$(4,9)^+$	D	B	$(4,9)^+$	D	B	$(4,9)^+$
	W	C	$(4,9)^+ \cdot C_4H_{10}$	W	C	$(4,9)^+ \cdot C_4H_8$	W	C	$(4,9)^+ \cdot C_4H_6$
	W	C	$(4,10)^+ \cdot C_4H_{10}$	W	C	$(4,10)^+ \cdot C_4H_8$	W	C	$(4,10)^+ \cdot C_4H_6$
(5,11)	W	C	$(5,11)^+ \cdot C_2H_4$	D	C	$(5,11)^+ \cdot C_4H_8$	D	C	$(5,11)^+ \cdot C_4H_6$
	D	C	$(5,11)^+ \cdot C_4H_{10}$						
(5,12)	W	C	$(5,11)^+$	W	C	$(5,11)^+$	W	C	$(5,11)^+$
	M	C	$(5,12)^+ \cdot C_2H_4$	M	C	$(5,12)^+ \cdot C_2H_4$	W	C	$(5,11)^+ \cdot C_4H_4$
	D	C	$(5,12)^+ \cdot C_4H_{10}$	D	C	$(5,12)^+ \cdot C_4H_8$	D	A	$(5,12)^+ \cdot C_4H_6$
(5,13)	D	C	$(5,11)^+$	D	B	$(5,11)^+$	M	C	$(5,11)^+$
	W	C	$(5,12)^+$	M	C	$(5,12)^+$	M	C	$(5,12)^+$
	W	C	$(5,11)^+ \cdot C_4H_{10}$	W	C	$(5,13)^+ \cdot C_4H_8$	W	C	$(5,12)^+ \cdot C_4H_6$
	W	C	$(5,12)^+ \cdot C_4H_{10}$				D	B	$(5,13)^+ \cdot C_4H_6$
	W	C	$(5,13)^+ \cdot C_4H_{10}$						
(6,13)	D	C	$(6,13)^+ \cdot C_4H_{10}$	D	C	$(6,13)^+ \cdot C_4H_8$	D	C	$(6,13)^+ \cdot C_4H_6$
(6,14)	W	C	$(6,13)^+$	W	C	$(6,13)^+$	W	C	$(6,13)^+$
	D	C	$(6,14)^+ \cdot C_4H_{10}$	D	C	$(6,14)^+ \cdot C_4H_8$	D	C	$(6,14)^+ \cdot C_4H_6$
(6,15)	M	C	$(6,13)^+$	M	C	$(6,13)^+$	M	B	$(6,13)^+$
	D	B	$(6,14)^+$	D	A	$(6,14)^+$	D	A	$(6,14)^+$
	W	C	$(6,13)^+ \cdot C_4H_{10}$	W	C	$(6,14)^+ \cdot C_4H_8$	W	C	$(6,14)^+ \cdot C_4H_6$
	W	C	$(6,14)^+ \cdot C_4H_{10}$	W	C	$(6,15)^+ \cdot C_4H_8$	W	C	$(6,15)^+ \cdot C_4H_6$
(7,16)	D	C	$(7,16)^+ \cdot C_4H_{10}$	D	C	$(7,16)^+ \cdot C_4H_8$	D	C	$(7,16)^+ \cdot C_4H_6$
(7,17)	W	C	$(7,16)^+$	W	C	$(7,16)^+$	W	C	$(7,16)^+$
	D	C	$(7,17)^+ \cdot C_4H_{10}$	D	C	$(7,17)^+ \cdot C_4H_8$	D	B	$(7,17)^+ \cdot C_4H_6$
(7,18)	W	C	$(7,16)^+$	M	C	$(7,16)^+$	W	C	$(7,16)^+$
	W	C	$(7,17)^+$	W	C	$(7,17)^+$	W	C	$(7,17)^+$
	D	C	$(7,18)^+ \cdot C_4H_{10}$	D	C	$(7,18)^+ \cdot C_4H_8$	D	B	$(7,18)^+ \cdot C_4H_6$

[a] These columns represent the product intensity with respect to the other peaks in that particular spectrum with each product marked as the dominant (D) product of the reaction or as strong (S), moderate (M), or weak (W) product ions. [b] These columns represent the product intensity with respect to all of the cluster reactions studied with each product marked as strong (A), moderate (B), or weak (C).

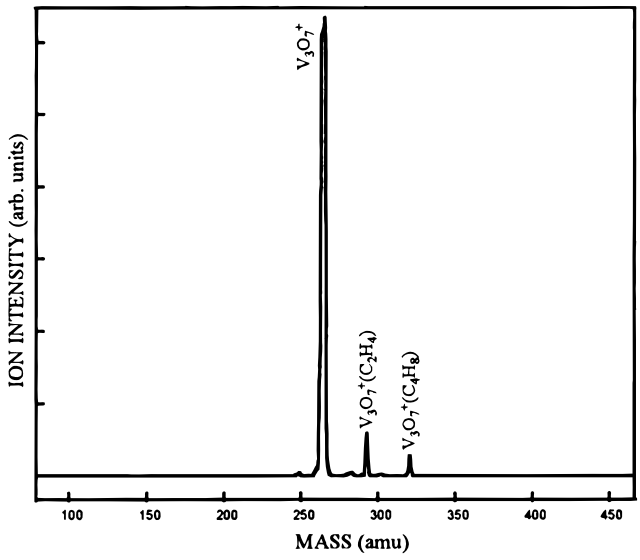

Figure 4. Spectra of reaction $V_3O_7^+$ with 0.2 mTorr 1-butene displays predominant C−C cracking.

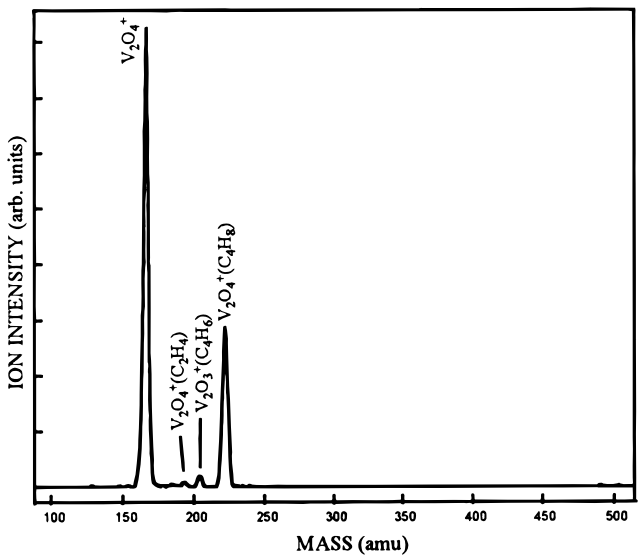

Figure 5. Spectra of reaction of $V_2O_4^+$ with 0.2 mTorr of 1,3-butadiene displays channels for both dehydration of association product and C−C cracking.

It is interesting to compare the reactions of 1,3-butadiene with those of the other hydrocarbons. The majority of the clusters studied display molecular association of 1,3-butadiene as the dominant reaction pathway, in addition to the abstraction of oxygen from the clusters as seen with the other two hydrocarbons. The nonselectivity of the clusters $V_2O_{4,5}^+$ was exhibited once more, with minor channels corresponding to both C−C cracking, as well as dehydration of the association product, i.e., H_2O loss from $V_2O_4^+ \cdot C_4H_8$ as seen in the spectrum in Figure 5. $V_3O_7^+$ was more specific and displayed a dominant dehydration product as observed in Figure 6, but the only reaction for the cluster $V_3O_6^+$ was association. Implications of the reactivities of these vanadium oxide clusters with the aforementioned hydrocarbons are discussed later. Evidently, a combination of the effects of exposed available metal sites and the oxidation states of the vanadium atoms are exemplified by these experiments and give insight into the reactions of these

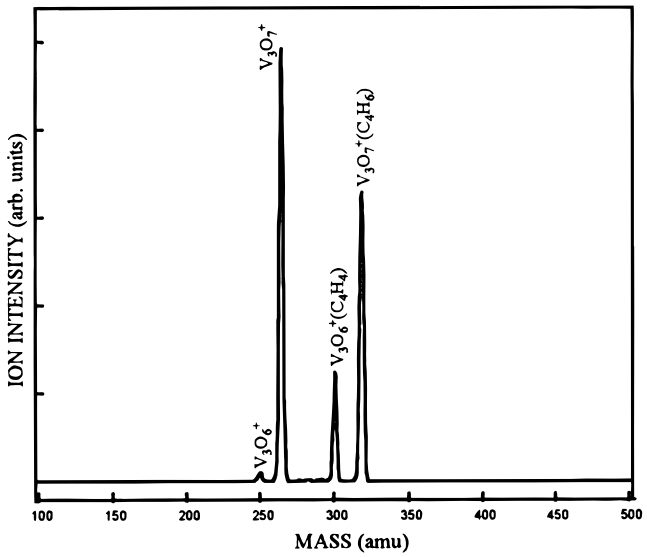

Figure 6. Spectra of reaction of $V_3O_7^+$ with 0.2 mTorr of 1,3-butadiene displays predominant dehydration of the association product.

clusters. The reactivities of selected vanadium oxide clusters with various reactants are summarized in Tables 3 and 4.

Discussion

The mass distribution pattern of vanadium oxide clusters obtained in the present studies shows that the dominant clusters can be represented by $(VO_2)_n(V_2O_5)_m(O_2)_{0-2}^+$. Vanadium is a group V transition metal with an electronic structure of [Ar]-$3d^34s^2$. Bulk vanadium oxide with the stoichiometry of V_2O_5 is an ionic compound, in which both vanadium atoms are in the +5 oxidation state. Accordingly, such clusters as VO_2^+, $V_3O_7^+$, $V_5O_{12}^+$, and $V_7O_{17}^+$ should be very stable clusters. Indeed, the results from the current experiments support this, but as will be seen, the clusters $V_3O_7^+$ and $V_5O_{12}^+$ display reactive selectivity not seen with any of the other clusters studied.

The mass distribution in Figure 1a has two features that need to be addressed. First, the distribution displays a progression toward a greater oxygen-to-metal ratio with respect to the first cluster in a series, as the number of vanadium atoms in the cluster series increases. Second, a trend is seen for a greater intensity for the oxygen-rich clusters in the series containing even numbers of metal atoms as compared to the series having odd numbers of vanadium atoms. These two occurrences can be explained by examining the possible structures of these clusters and the oxidation states of the vanadium atoms in each structure. The prominent peaks in the first series, as seen in Figure 1b, are VO^+ and VO_2^+ with peaks of a higher oxygen content being present, but to a much lesser degree. These clusters also appear in Figure 1a but cannot be seen in the scale of this spectrum due to their low intensities. If the clusters are thought of as being ionic in nature, the vanadium atoms in these two cations have +3 and +5 oxidation states, respectively. It is postulated that the clusters of higher oxygen content (for example, VO_3^+, VO_4^+, etc.) are the VO^+ and VO_2^+ clusters with molecular oxygen attached, although the low intensity of these peaks did not allow for CID experiments to be performed in order to determine whether O_2 units are lost at near thermal energies.

The next series begins with the cluster $V_2O_4^+$ where the oxidation states of the vanadium atoms can be thought of as (+4,+5), although this cluster may exhibit a mixed valency.

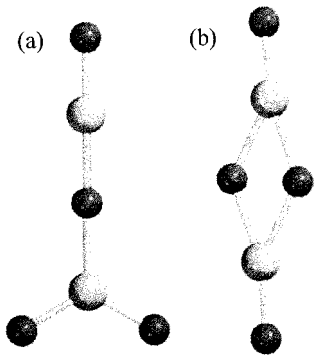

Figure 7. Proposed structures for the cluster $V_2O_4^+$.

However, for the purpose of this discussion, each atom will be assigned an individual oxidation state. The proposed structures for $V_2O_4^+$ can be seen in Figure 7; the structures chosen for these and other clusters will be discussed in detail later. For the cluster $V_2O_4^+$, coordinative unsaturation would allow for more molecular oxygen to be adsorbed to its surface. Coordinative unsaturation arises from the fact that only a limited number of ligands can be within bonding distance of a metal atom or ion due to steric and electronic effects.[28] In the case of the cluster $V_2O_4^+$, it is postulated that coordinative unsaturation occurs due to the available oxidation states of the cluster. For the clusters with additional oxygen, the oxidation states of certain vanadium atoms would be in the +6 state if all the oxygen atoms were directly bonded to the vanadium atoms, but the V^{6+} is an unstable oxidation state. Therefore, it is proposed that the cluster $V_2O_6^+$ is composed of the more stable cluster $V_2O_4^+$ with molecular oxygen adsorbed to the surface.

The cluster $V_2O_5^+$, however, demonstrates an unusual CID fragmentation pattern compared to all the other clusters studied. Unlike the other oxygen-rich clusters which lose O_2 near thermal energies, the $V_2O_5^+$ first loses a single oxygen atom at slightly elevated energies (~1 eV center-of-mass reference frame) and then begins to lose an O_2 unit as well after approximately 2 eV center-of-mass reference frame of energy is added to the cluster under single-collision CID conditions. There are two possible explanations for these findings. For $V_2O_5^+$ to lose molecular oxygen, the cluster $V_2O_3^+$ would be formed with oxidation states of +3 and +4. Although this cluster is seen in the spectra at very low concentrations, it is not observed in Figure 1a,b due to the ion intensity range of these spectra. Under the conditions in which these clusters are formed, clusters that have a vanadium atom in the +3 oxidation state are not favored. For example, the cluster $V_4O_8^+$ has two possible structures. A straight-chain backbone of V−O− units would allow all the vanadium atoms to be in the +4 or +5 states. However, the other possible structure that allows for the branching of the cluster must have one of the vanadium atoms in a +3 state, and the intensity of this peak begins to diminish compared to the lower mass clusters which have strong peaks for clusters with a 1:2 metal-to-oxygen ratio. The possible structures for $V_5O_{10}^+$ all have at least one vanadium atom in the +3 oxidation state, and this cluster is not observed in the spectra; see Figure 1. Therefore, formation of clusters with a +3 oxidation state are less favored then those clusters that have all the vanadium atoms with a combination of +4 and +5 oxidation states.

Another factor that may play a role in the unique fragmentation pattern of the cluster $V_2O_5^+$ may be to the manner in which the O_2 unit is adsorbed. Due to the electronegativity of oxygen, electron transfer from the transition metal oxide to the adsorbed oxygen commonly occurs, although it may not be a necessary condition for chemisorption to occur.[29] However, studies

conducted on supported V_2O_5 indicate that the adsorbed molecular oxygen does result in the transfer of an electron to form the superoxide ion (O_2^-).[30] For these reasons, it is believed that the adsorption of O_2 on the vanadium oxide clusters are of two types: chemisorption (possibly involving the transfer of an electron) and physical adsorption. All other oxygen-rich clusters that would allow for one or more vanadium atoms to be in a +6 oxidation state lose O_2 near thermal energies and are therefore thought to be comprised of molecular oxygen associated through physical adsorption or weak chemisorption. However, for $V_2O_5^+$ the O_2 unit is thought to be strongly chemisorbed to the cluster $V_2O_3^+$ due to the amount of energy (~2 eV) needed to break this bond. For these reasons, the cluster $V_2O_5^+$ is unusual compared to the rest of the clusters present in the mass distribution. It is believed that the more strongly adsorbed molecular oxygen of the $V_2O_5^+$ cluster allows for the loss of a single oxygen atom due to a greater exchange of electron density between the metal and oxygen, whereas the other oxygen-rich clusters which display facile O_2 loss are thought to be bonded to a lesser degree.

As mentioned previously, the oxygen-rich clusters ($V_2O_6^+$, $V_3O_{8,9}^+$, $V_4O_{10}^+$, $V_5O_{13}^+$, $V_6O_{15}^+$, and $V_7O_{18}^+$) all lose O_2 near thermal energies as seen in the CID results presented in Tables 1 and 2. The adsorption of O_2 onto these clusters appears to be a physical adsorption or weak chemisorption. From the proposed structures, the oxidation states of the vanadium atoms for the even series are lower than for those of the odd numbered series. Therefore, the adsorption of a greater number of O_2 units is more favorable for the less coordinated even series with lower oxidation states than for the less coordinated odd series which have slightly higher oxidation states. This is evidenced by the mass distribution which generally displays a greater intensity for oxygen-rich species within an even series. In addition, the smaller clusters (i.e., $V_{2-7}O_y^+$) display a greater number of peaks within a series that have an even number of vanadium atoms as compared to the series that contain an odd number of vanadium atoms. For those clusters that are already in a high oxidation state (all vanadium atoms already in the +5 state), adsorption occurs to a lesser degree as evidenced by the mass distribution that displays these clusters (e.g., $V_3O_9^+$, $V_5O_{14}^+$, $V_7O_{19}^+$, and $V_9O_{24}^+$) which are minor in comparison to the other peaks in the mass distribution.

The $V_3O_y^+$ series begin with the clusters $V_3O_6^+$ and $V_3O_7^+$ where their oxidation states may be viewed as (+4, +4, +5) and (+5, +5, +5), respectively, with the proposed structures shown in Figures 2 and 3. The only other major peak in this series is $V_3O_8^+$ which can be viewed as a $V_3O_6^+$ with an associated O_2 unit; in fact, the CID of this cluster leads to molecular oxygen loss at near thermal energies. As stated previously, the $V_3O_7^+$ with the vanadium atoms already in a +5 oxidation state are less inclined to associate additional oxygen molecules. This is evidenced by the observation that the mass distribution shows a decrease in intensity for the cluster $V_3O_9^+$, and CID of this cluster displays O_2 loss at near thermal energies. These trends continue as the number of vanadium atoms in each series progress. For the odd-numbered series, the clusters VO_2^+, $V_3O_7^+$, $V_5O_{12}^+$, $V_7O_{17}^+$, and $V_9O_{22}^+$ all display structures that allow for every vanadium atom to be in the +5 oxidation state. There are no possible structures for the series with an even number of vanadium atoms that have the +5 oxidation state for all the metal atoms. Clusters of higher oxygen content that do not fit the formula $(VO_2)_n(V_2O_5)_m(O_2)_q^+$ (with $n \geq 1$ and $q = 0$) lose molecular oxygen near thermal energies and single-collision conditions. For example, the cluster $V_3O_9^+$ has the values of $n = 1$, $m = 1$, and $q = 1$, (therefore, $q \neq 0$), and the cluster loses molecular oxygen. Although clusters with stoichometries of $(V_2O_5)_m$ are stable as neutral molecules, as cations (with one fewer electron) they are unstable because one of the vanadium atoms would be in the +6 oxidation state if all the oxygen were bonded to the vanadium with no O−O bonds present. But unlike the $V_2O_5^+$ species, there are structures for the clusters $V_4O_{10}^+$ and $V_6O_{15}^+$ that allow the loss of O_2 units, without placing any of the vanadium atoms in the +3 state.

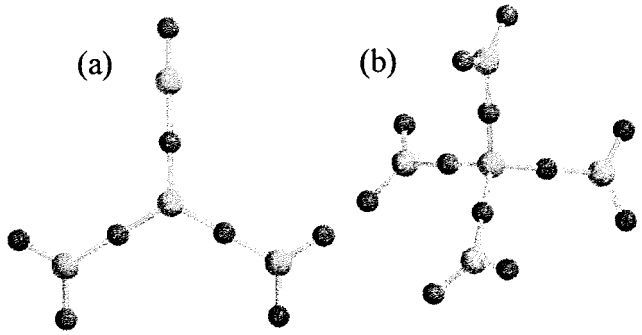

Figure 8. A single structural arrangement for each of the clusters $V_4O_8^+$ and $V_5O_{12}^+$.

The second trend in the mass distribution, namely the observed shift to higher oxygen content as the number of vanadium atoms in the cluster series increases, can be attributed to the ability of the clusters to form branched structures. Beginning at the cluster series with four vanadium atoms, branching may occur. Examples of this can be seen in Figure 8 which displays a single structural arrangement for each of the clusters, $V_4O_8^+$ and $V_5O_{12}^+$. The branching allows for higher coordination of the branched vanadium atoms which increases the number of oxygen atoms that may be bonded to the cluster. As the degree of branching increases, the cluster series shift from the 1:2 metal-to-oxygen ratio (i.e., $V_2O_4^+$ and $V_3O_6^+$) seen at the beginning of the mass distribution to a ratio with higher oxygen content (i.e., $V_{10}O_{22}^+$ and $V_{11}O_{24}^+$) for the first cluster of a series.

Since both vanadium and niobium are group VA transition metals, one might expect that similar formation patterns, dissociation patterns, and reactivities would result. However, these expectations are not observed in the comparison between these and prior studies.[23] With regard to the previous findings for niobium oxide clusters, the key building blocks and neutral dissociation products are comprised of both NbO_2 and NbO_3 units.[23] With only subtle differences, the present studies show similar CID results, as summarized in Tables 1 and 2, to those seen for the niobium oxide cluster cations. However, there is a difference between clusters composed of these two transition metal species. In comparing the mass distributions of the niobium and vanadium oxide clusters, each series in the niobium mass distribution begins with $M_xO_y^+$, whereas each series for the vanadium oxide mass distribution (Figure 1) begins with $M_xO_{y-1}^+$, i.e., with one less oxygen atom. The oxide cluster distributions for niobium and vanadium may differ because of the stable oxidation states of the two elements. The stable oxidation states of niobium are the +3 and +5, whereas the stable states of vanadium are +2, +3, +4, and +5, with the +5 state being the most stable for both metals. Therefore, the niobium clusters that would have metal atoms in the +4 state, at a metal-to-oxygen ratio of 1:2, would be unstable and are not seen in the mass distribution.[23] The vanadium atoms, on the other hand, are stable in the +4 state, and therefore these

clusters are among those observed. The stable oxidation states for niobium would also account for the fact that molecular oxygen is not lost for the clusters $Nb_3O_8^+$ and $Nb_4O_{10}^+$ as seen for the vanadium clusters with the same stoichiometry; this loss would result in clusters with a niobium atom in the unstable +4 oxidation state.

Collision-induced dissociation (CID) has proven to be a valuable method for determining structures of a variety of molecules.[31] Results of studies conducted here, and summarized in Tables 1 and 2, show the selected clusters and their CID products. The listings are in order of increasing relative bond dissociation energy for each cluster type with the lowest dissociation energy listed first. From these results, several trends can be observed. For example, fragment units of $(VO_2)_x(VO_3)_y$ are commonly observed for metal-rich clusters, but only after substantial energy (about 3−5 eV center-of-mass frame) has been added; however, oxygen-rich clusters can lose O_2 near thermal energies as discussed previously.

CID studies of the smaller clusters $V_{2-4}O_y^+$ (Table 1) and the larger clusters $V_{5-7}O_y^+$ (Table 2) suggest that these structures are comprised entirely of V−O bonds without the presence of V−V bonds. This is not surprising in view of the fact that it has been observed that the V−O bond (149 kcal/mol)[32,33] and the V^+−O bond (131 kcal/mol)[34,35] are approximately 2−2.5 times stronger than the V−V bond (63 kcal/mol).[36−39] Details about the structures and types of bonding (i.e., V−O−O vs V associated with the double bond of O_2) in the oxygen-rich clusters, such as $V_2O_{6-8}^+$, $V_3O_{8,9}^+$, and $V_4O_{10-12}^+$, are still undetermined although there is a facile O_2 loss in these clusters.

The proposed structures of $V_2O_4^+$ are displayed in Figure 7. Structures with V−V and O−O bonds are not thermodynamically favorable as discussed previously and are not addressed here. Although the isomer shown in Figure 7b may exist to some extent, it is unlikely to be of importance in view of the fact that two bonds would need to be broken to form the CID products observed, namely VO_2^+ and VO^+.

In comparing the structures of $V_3O_6^+$ and $V_3O_7^+$, it is observed that their reactivities, which are remarkably different, may be influenced significantly by cluster structure and oxidation states of the vanadium atoms. In the case of $V_3O_6^+$, the CID fragmentation products in order of increasing bond dissociation energies of the original cluster are VO^+, $V_2O_4^+$, and VO_2^+. These fragments can be accounted for by the structure proposed in Figure 2a. If the structure in Figure 2b were present, the fragment VO_2^+ would be more prevalent and VO^+ would occur to a lesser extent if at all. However, this structure and one that would incorporate the ring structure proposed for the $V_2O_4^+$ cluster (Figure 2c) cannot be totally ruled out as possible isomers that may be present to a minor extent. Another possible structure, Figure 2d, is a large ring composed of three vanadium atoms and three oxygen atoms with an additional oxygen atom bonded to each of the metal sites.

On the other hand, $V_3O_7^+$ is unique in the fact that VO_2^+, not the VO^+ unit, is the dominant fragmentation channel, as illustrated in Table 1. Under multicollision conditions and approximately 5 eV (center-of-mass reference frame), VO^+ is observed in the spectra. This can be postulated as a loss of two VO_3 units which can be rationalized from the predicted structure in Figure 3a. Again, a ring structure similar to that for $V_2O_4^+$ may be present to a minor extent as an isomer for this cluster as shown in Figure 3b. Another possible structure is that for a ring containing three vanadium atoms and four oxygen atoms which is shown in Figure 3c, unlike that for $V_3O_6^+$ which was mentioned previously.

The vanadium oxide clusters studied have shown little activity toward saturated hydrocarbons. The main products formed for all the clusters studied were the association product and abstraction of atomic and molecular oxygen from certain clusters as discussed previously. The clusters $V_2O_{4,5}^+$, $V_3O_{6,7}^+$, and $V_5O_{11,12}^+$ all demonstrated a minor pathway for the C2−C3 cracking upon reaction with *n*-butane. This reaction process was evidently due to the thermodynamic favorability of formation of two ethyl groups rather than methyl and propyl groups. In addition, minor products representing the dehydration of the $V_2O_{4,5}^+$ association products were also observed. These two clusters displayed several channels for reactivity but have shown no selectivity for their reaction pathways.

Another unique reaction pathway observed for reactions of the vanadium oxide clusters with the three hydrocarbons studied is the loss of a single oxygen at near thermal energies and single-collision conditions. None of the clusters studied were observed to lose a single oxygen atom at various energies under CID conditions with the exception of $V_2O_5^+$. This oxygen loss may be attributed to the oxygenation of the neutral hydrocarbon upon reaction with the selected cluster. The loss of O_2 from the oxygen-rich species at single-collision conditions near thermal energies may be the result of a CID process, as these same reactions were observed for the CID experiments performed with xenon at single-collision conditions near thermal energies.

The reaction of 1-butene with these clusters demonstrated more interesting results. Association dominated the reaction pathway for most of these clusters with the same phenomena occurring with the loss of both molecular and atomic oxygen near thermal energies for particular clusters. The clusters $V_2O_{4,5}^+$, $V_3O_7^+$, and $V_5O_{12}^+$ were all able to react, producing a C2−C3 cracking product. However, the clusters $V_2O_{4,5}^+$ were both less reactive and less selective compared to the other two clusters. The reaction of these species with 1-butene also displayed dehydration products, association products $V_2O_{4,5}^+ \cdot C_4H_6$, and the cracking product $V_2O_4^+ \cdot CH_2$ in addition to the C2−C3 cracking product $V_2O_{4,5}^+ \cdot C_2H_4$ mentioned. Although the cluster $V_3O_7^+$ displayed a dominant cracking channel, minor dehydration of the association product was also observed. In comparing the clusters $V_3O_6^+$ and $V_3O_7^+$ with 1-butene, the effects incurred by the presence of the extra oxygen atom are evident. The reaction channels were entirely molecular association for $V_3O_6^+$, but reactions of $V_3O_7^+$ displayed C2−C3 cracking of the single bond of 1-butene. The reaction scheme of $V_3O_7^+$ with 1-butene can be described as follows:

$$V_3O_7^+ + C_4H_8 \rightleftharpoons V_3O_7^+ \cdot C_4H_8 \quad (1)$$

$$\rightleftharpoons V_3O_7^+ \cdot C_2H_4 + C_2H_4 \quad (2)$$

where the reaction process results in the formation of two C_2H_4 units. It should be stressed that the studies of the reactions of both $V_3O_6^+$ and $V_3O_7^+$ were conducted under similar conditions near thermal energies. Comparing the results in Figures 9 and 10 illustrates the differences in the reactivities of these two clusters. The C2−C3 cracking with $V_3O_7^+$ may be a result of the favorability of breaking the α C−C bond of butene. These same arguments may be made for the reactivities of the cluster $V_5O_{11}^+$ and $V_5O_{12}^+$, where $V_5O_{11}^+$ is totally inert to the bond breaking of 1-butene. Cracking of alkenes occurs industrially upon reacting with highly oxidative compounds such as O_3

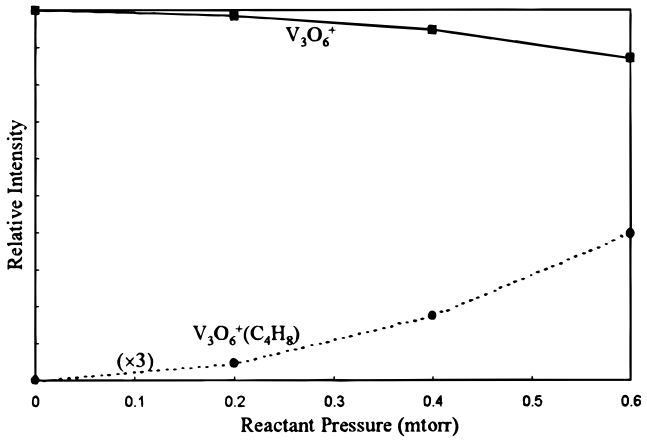

Figure 9. Plot of product branching ratios of the reactivities of $V_3O_6^+$ with 1-butene.

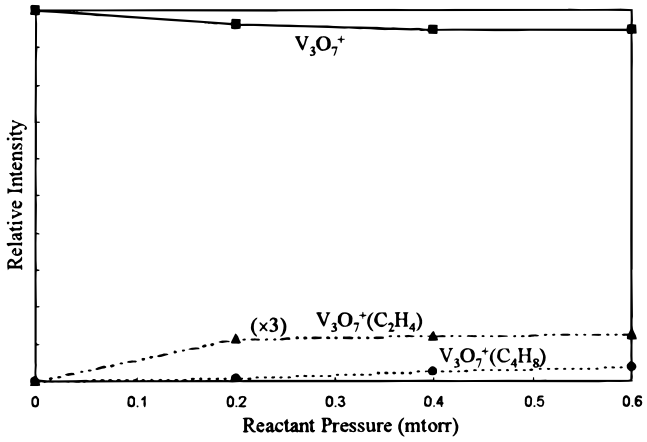

Figure 10. Plot of product branching ratios of the reactivities of $V_3O_7^+$ with 1-butene.

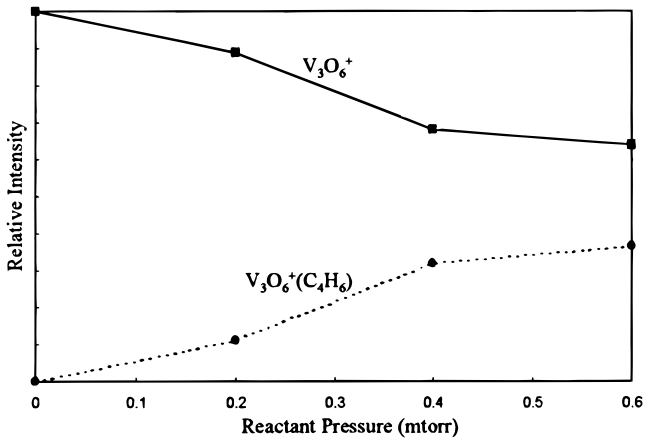

Figure 11. Plot of product branching ratios of the reactivities of $V_3O_6^+$ with butadiene.

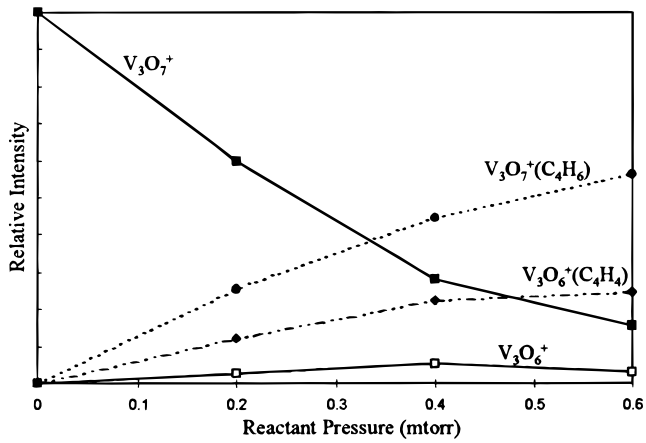

Figure 12. Plot of product branching ratios of the reactivities of $V_3O_7^+$ with butadiene.

(ozonolysis process) or $KMnO_4$,[40] and it is interesting to observe that this process occurs only with specific vanadium oxide cluster ions.

The reaction with 1,3-butadiene with the clusters studied again displays the association channel as the dominant pathway for most of these clusters. The same oxygen abstraction reactions occurred for these clusters as was seen previously. The major differences between the niobium and vanadium oxide cluster cations are seen by comparing their reactions with the hydrocarbon 1,3-butadiene (C_4H_6). The reactions of the other hydrocarbons studied here were not conducted for the niobium oxide cluster cations. For the reactions of niobium oxide cluster cations with 1,3-butadiene,[23] molecular association products ($Nb_xO_y^+ \cdot C_4H_6$), loss of atomic oxygen ($Nb_xO_{y-1}^+$), and association of butadiene with these products ($Nb_xO_{y-1}^+ \cdot C_4H_6$) were observed for the specific clusters $Nb_3O_{8-9}^+$ and $Nb_4O_{11}^+$. By contrast, the clusters $V_2O_{4,5}^+$ were able to react to form minor products for C2−C3 cracking and dehydration products in addition to the dominant pathway of molecular association. The cluster $V_3O_7^+$ demonstrates a higher degree of selectivity, producing only the dehydration and association products with no cracking products and only minor oxygen abstraction observed. The $V_5O_{12}^+$ also displays a minor channel for the dehydration product, whereas, $V_5O_{11}^+$ is only able to associate 1,3-butadiene. The special nature of the reactivities of the $V_3O_7^+$ cluster toward butadiene can be described in terms of the coordination of the extra oxygen atom onto the $V_3O_6^+$ cluster, which is only able to associate this reactant. The reactivities of these two clusters can be seen in Figures 11 and 12, which display the branching ratios in terms of intensity versus pressure of reactant gas. As mentioned earlier, the structures and oxidation states of $V_3O_6^+$ and $V_3O_7^+$ are predicted to account for the changes in reactivity.

In considering the reactions of $V_3O_7^+$ with butadiene, the reaction process can be described as follows

$$V_3O_7^+ + C_4H_6 \Rightarrow V_3O_7^+ \cdot C_4H_6 \quad (3)$$

$$\Rightarrow V_3O_6^+ \cdot C_4H_4 + H_2O \quad (4)$$

where the first channel is molecular association and the second channel is dehydration of $V_3O_7^+ \cdot C_4H_6$. The product $V_3O_6^+ \cdot C_4H_4$ involves dehydrogenation, and perhaps rearrangement, of butadiene; in fact, it is postulated that the structure resembles $V_3O_5^+ \cdot C_4H_4O$, where C_4H_4O has a structure similar to furan, which is associated to the $V_3O_5^+$ cluster surface. Formation of organic compounds from the reactions of 1,3-butadiene with oxygen-containing compounds is highly exothermic, and formation of furan-like intermediates from butadiene-like precursors in their reactions with vanadium phosphorus oxides has been proposed.[14] The ability of certain vanadium oxide clusters to oxidize hydrocarbons into oxygen-containing neutral products is supported by the above reaction process. Also, the occurrence of oxidation (shown here as dehydration of $V_3O_7^+ \cdot C_4H_6$) is supportive of an oxygen-mediated reaction process.

It should be stressed that the reactivities of $V_3O_6^+$ and $V_3O_7^+$ are different, not only in terms of their reaction channels but also in their extent of reaction with different species. Table 3

provides a summary of selected vanadium oxide cluster ion reaction products. These observations imply that the reactivities of $V_3O_7^+$ with hydrocarbons are even more unique. Reactions of $V_3O_6^+$ are proposed to proceed through a metal center, but for the case of $V_3O_7^+$, the extra oxygen atom significantly changes its reactivities toward hydrocarbons. Even though it is believed that the reactions of this cluster are also metal-mediated, active involvement of the oxygen ligand most likely occurs.

Conclusions

Reactivities and collision-induced dissociation (CID) of vanadium oxide cluster ions were investigated on a triple quadrupole mass spectrometer coupled with a laser vaporization source. It was found that VO_2 and V_2O_5 units, or alternatively VO_2 and VO_3 units, are the building blocks, as demonstrated by both the cluster formation and CID processes. Collision-induced dissociation with the aid of ab initio calculations leads to insights into the possible structures of vanadium oxide clusters. Conversely, the additional oxygen atom in a cluster such as $V_3O_7^+$ is the reactive site in the hydrocarbon reactions. In particular, the reactions of $V_3O_7^+$ and $V_5O_{12}^+$ toward butadiene and 1-butene are found to differ significantly from similar reactions toward $V_3O_6^+$ and $V_5O_{11}^+$ and also proceed through dehydration and C−C cracking, respectively. The greater reactivity with hydrocarbons of $V_3O_7^+$ and $V_5O_{12}^+$, which evidently both consist entirely of vanadium in the +5 oxidation state, compared to $V_3O_6^+$ and $V_5O_{11}^+$, is revealing both of the role of the extra oxygen atom and of the oxidation state of the vanadium atoms which may be indicative of the crucial role played by V^{5+} in heterogeneous oxidation catalysis.[41] However, the reactivity of the clusters appeared to display a size dependence. For the clusters with all vanadium atoms in the +5 oxidation state, i.e., $V_3O_7^+$, $V_5O_{12}^+$, and $V_7O_{17}^+$, the reactivity decreased until the cluster $V_7O_{17}^+$, which evidently is inert to cracking and dehydration of these hydrocarbons and displayed only association and oxygen abstraction products. These studies have demonstrated the importance of oxidation state, structure, and cluster size on the reactivity and selectivity of the vanadium oxides cluster cations reactions with the various hydrocarbons studied.

Acknowledgment. Financial support from the DuPont Company and a Goali grant from the National Science Foundation, Grant CHE-9632771, is greatly appreciated. We wish to thank Dr. David Thorn of the DuPont Company for helpful discussions during the course of this work.

References and Notes

(1) Imelik, B., Naccache, C., Coudurier, G., Praliaud, H., Meriaudeau, P., Gallezot, P., Martin, G. A., Vedrine J. C., Eds. *Metal-Support and Metal Additive Effects in Catalysis*; Elsevier: Amsterdam, 1982.
(2) Bond, G. C.; Tahir, S. F. *Appl. Catal.* **1991**, *71*, 1.
(3) Ramírez, R.; Casal, B.; Utrera, L.; Ruiz-Hitzky, E. *J. Phys. Chem.* **1990**, *94*, 8960.
(4) Legrouri, A.; Baird, T.; Fryer, J. R. *J. Catal.* **1993**, *140*, 173.
(5) Ivanenko, S. V.; Dzhoraev, R. R. *Russ. J. Appl. Chem.* **1995**, *68*, 849.
(6) Bond, G. C. *J. Catal.* **1989**, *116*, 531.
(7) Andersson, A.; Lundin, S. T. *J. Catal.* **1979,** *58*, 383.
(8) Deo, G.; Wachs, I. E. *J. Catal.* **1994**, *146*, 323.
(9) Chen, S. Y.; Willcox, D. *Ind. Eng. Chem. Res.* **1993**, *32*, 584.
(10) Oyama, S. T.; Somorjai, G. A. *J. Phys. Chem.* **1990**, *94*, 5022.
(11) Tran, K.; Hanning-Lee, M. A.; Biswas, A.; Stiegman, A. E.; Scott G. W. *J. Am. Chem. Soc.* **1995**, *117*, 2618.
(12) Topsøe, N.-Y. *Science* **1994**, *265*, 1217.
(13) Centi, G.; Trifirò, F.; Ebner, J. R.; Franchetti, V. M. *Chem. Rev.* **1988**, *88*, 55. (b) Centi, G. *Catal. Today* **1993**, *16*, 5.
(14) Haggin, J. *Chem. Eng. News* **1995**, *73*, 20.
(15) Rhodin, T. N., Ertl, G., Eds. *The Nature of the Surface Chemical Bond*; North-Holland: New York, 1979; Chapter 2.
(16) Kappes, M. M.; Staley, R. H. *J. Am. Chem. Soc.* **1981**, *103*, 1286.
(17) Eller, K.; Schwarz, H. *Chem. Rev.* **1991**, *91*, 1121. (b) Schröder, D.; Schwarz, H. *Angew. Chem., Int. Ed. Engl.* **1995**, *34*, 1973 and references therein.
(18) Weisshaar, J. C. *Acc. Chem. Res.* **1993**, *26*, 213.
(19) Jackson, T. C.; Carlin, T. J.; Freiser, B. S. *J. Am. Chem. Soc.* **1986**, *108*, 1120.
(20) Guo, B. C.; Kerns, K. P.; Castleman, Jr., A. W. *Int. J. Mass Spectrom. Ion Processes* **1992**, *117*, 129.
(21) Yu, W.; Freas, R. B. *J. Am. Chem. Soc.* **1990**, *112*, 7126.
(22) Fialko, E. F.; Kikhtenko, A. V.; Goncharov, V. B.; Zamaraev, K. I. *J. Phys. Chem. A* **1997**, *101*, 5772, 8607.
(23) Deng, H. T.; Kerns, K. P.; Castleman, Jr., A. W. *J. Phys. Chem.* **1996**, *100*, 13386.
(24) Kerns, K. P.; Guo, B. C.; Deng, H. T.; Castleman, Jr., A. W. *J. Chem. Phys.* **1994**, *101*, 8529.
(25) Kerns, K. P.; Guo, B. C.; Deng, H. T.; Castleman, Jr., A. W. *J. Phys. Chem.* **1996**, *100*, 16817.
(26) Greenwood, N. N.; Earnshaw, A. *Chemistry of the Elements*, 1st ed.; Pergamon Press: Oxford, 1984; Chapter 22.
(27) Hehre, W. J.; Burke, L. D.; Shusterman, A. J. *Spartan Software*; Wavefunction, Inc.: Irvine, CA, 1994.
(28) Kung, H. H. *Transition Metal Oxides, Surface Chemistry and Catalysis*; Elsevier: New York, 1989.
(29) Bielanski, A.; Haber, J. *Oxygen in Catalysis*; Marcel Dekker: New York, 1990; Chapter 2. (b) Henrich, V. E.; Cox, P. A. *The Surface Science of Metal Oxides*; Cambridge University Press: New York, 1994; Chapter 6.
(30) Shvets, V.; Vorotyntsev, V.; Kazansky, V. *Kinet. Catal.* **1969**, *10*, 356.
(31) Boyd, R. K. *Mass Spectrom. Rev.* **1994**, *13*, 359.
(32) Balducci, G.; Gigli, G.; Guido, M. *J. Chem. Phys.* **1983**, *79*, 5616.
(33) Pedley, J. B.; Marshall, E. M. *J. Phys. Chem. Ref. Data* **1983**, *12*, 967.
(34) Aristov, N.; Armentrout, P. B. *J. Am. Chem. Soc.* **1984**, *106*, 4065.
(35) Kappes, M. M.; Staley, R. H. *J. Phys. Chem.* **1981**, *85*, 942.
(36) Kant, A.; Lin, S.-S. *J. Chem. Phys.* **1969**, *51*, 1644.
(37) Langridge-Smith, P. R. R.; Morse, M. D.; Hansen, G. P.; Smalley, R. E.; Merer, A. J. *J. Chem. Phys.* **1984**, *80*, 593.
(38) Spain, E. M.; Morse, M. D. *Int. J. Mass Spectrom. Ion Processes* **1990**, *102*, 183; *J. Phys. Chem.* **1992**, *96*, 2479.
(39) Su, C.-X.; Hales, D. A.; Armentrout, P. B. *J. Chem. Phys.* **1993**, *99*, 6613.
(40) Wade, Jr., L. G. *Organic Chemistry*, 2nd ed.; Prentice Hall: Englewood Cliffs, NJ, 1991; Chapter 8.
(41) Coulston, G. W.; Bare, S. R.; Kung, H.; Birkeland, K.; Bethke, G. K.; Harlow, R.; Herron, N.; Lee, P. L. *Science* **1997**, *275*, 191.